



Contents list available at IJRED website

**International Journal of Renewable Energy Development**

Journal homepage: <https://ijred.undip.ac.id>



Research Article

# An investigation of a 3D printed micro-wind turbine for residential power production

Mohammad Shalby<sup>1\*</sup> , Ahmad A. Salah<sup>2</sup> , Ghayda' A. Matarneh<sup>1</sup> , Abdullah Marashli<sup>1</sup> ,  
Mohamed R. Gommaa<sup>1</sup> 

<sup>1</sup>Department of Mechanical Engineering, Faculty of Engineering, Al-Hussein Bin Talal University, Ma'an, Jordan

<sup>2</sup>Department of Electrical Engineering, Faculty of Engineering, Al-Hussein Bin Talal University, Ma'an, Jordan

**Abstract.** The wind energy sector is rapidly growing and has become one of the most important sources of renewable power production. New technologies are being developed to increase energy production. This study focuses on developing and evaluating a 3-D printed micro-wind turbine system for residential electricity production. The effectiveness of using Poly Lactic Acid material for model production was assessed using the SolidWorks environment. Then, three-dimensional CFD model was developed to simulate a micro-wind turbine. The CFD model was validated in good agreement against scale physical model experiments performed in a wind tunnel. The results demonstrated that the 5-blade micro-wind turbine design was the most effective under the tested conditions, with a low cut-in speed and the ability to operate under torque up to 70 N.m. Finally, the currently available manufacturing processes for micro-wind turbines have been evaluated. Future work should evaluate the performance of the MWT system under realistic conditions in a site test to determine energy production and total efficiency.

**Keywords:** Wind energy harvest, Low-speed wind turbine testing, Structural test, CFD, Model performance



@ The author(s). Published by CBIORE. This is an open access article under the CC BY-SA license (<http://creativecommons.org/licenses/by-sa/4.0/>).

Received: 20<sup>th</sup> Feb 2023; Revised: 25<sup>th</sup> March 2023; Accepted: 11<sup>th</sup> April 2023; Available online: 21<sup>st</sup> April 2023

## 1. Introduction

Global energy demand to grow 47% by 2050 (Gordon *et al.*, 2021). Thus, renewable will play an essential role in coping with growing energy needs for reducing fossil-fuel consumption and greenhouse gas emissions (Ajadi *et al.*, 2020; Aravindhan *et al.*, 2022). The world is experiencing an increase in the use of renewable sources of energy to restrain the effects of global climate change by decreasing the emission of CO<sub>2</sub> and increasing the security of the energy supply by reducing the proportion of use of fossil sources of energy especially with rising oil price (Lakatos *et al.*, 2011; Rehman *et al.*, 2023). The most actively developing areas of renewables are solar and wind generation (Li *et al.*, 2022; Roga *et al.*, 2022; Naqash *et al.*, 2021). However, wind power is one of the fastest-growing renewables segments due to its ability to generate large amounts of energy at competitive costs (Chaudhuri *et al.*, 2022). It constitutes more than 20% of the world's renewables and could reach up to 10 GW by 2030 (IRENA, 2022). The international installed wind energy capacity will experience a 30% compound annual growth rate (Scarabaggio *et al.*, 2021). This revolution was due to wind's vast potential and a decline in generation costs by one-third between 2008 and 2015 (Diógenes *et al.*, 2020). In 2020 the new wind power installations surpass 90 GW, growth by 53% compared to 2019, bring the total capacity of wind power to 743 GW. China, Asia Pacific was the largest regional market for new installations with 60%, USA, North America was the second regional market with 18.4%, in third was Europe with 15.9%,

replaced Latin America in the fourth regional market with 5.0%, followed by Africa and Middle East with 0.9% (Council, 2021; Sun *et al.*, 2021). Based on the power output, wind turbines can be classified as (large, medium, and small): large (>1 MW), medium (40 kW-1 MW), and small (<40 kW) (Spera David, 1995). Most wind power plants produce power by large horizontal wind axis wind turbines, usually deployed in locations with high wind quality and wind speeds of 6 m/s or more. A micro wind turbine (MWT) is a type of small-scale wind turbine used to generate electricity for residential or small commercial use (Wilberforce *et al.*, 2023). MWTs have gained popularity in recent years as a way to reduce energy costs and increase energy independence (Kumar & Prakash, 2023). Advances in blade design, control systems, and materials technology have improved the energy conversion efficiency of MWTs and reduced their cost (Ayhan & Sağlam, 2012). Advances in blade design, control systems, and materials technology have improved the energy conversion efficiency of MWTs and reduced their cost (Aljafari *et al.*, 2022; Aravindhan *et al.*, 2022; Carré *et al.*, 2022; Chudzik, 2023; Nijssen & Brøndsted, 2023; Raut *et al.*, 2017; Razzetti, 2022; Wu & Sun, 2018). These advancements have significantly increased the viability and popularity of MWTs as a renewable energy source and have paved the way for further developments in the future (Bangi *et al.* 2017). The wind speed is lower in places such as rooftops because of the high structure and houses (Clausen & Wood, 2000). In addition, the wind becomes highly turbulent at

\* Corresponding author

Email: [mohammad.shalby@ahu.edu.jo](mailto:mohammad.shalby@ahu.edu.jo) (M. Shalby)

this height, and the direction variation is significant. Therefore, unique MWT technology is needed to harvest wind energy over residential suburban dwellings' roofs (Tan *et al.*, 2022).

The electricity generated by MWTs can be stored in a battery that can later be used to power home electrical appliances. Although significant progress has been made in the wind energy sector, there is still potential for cost reduction and performance improvement of small (capacity <1 kW) wind turbines (Rao, 2019; Wilberforce *et al.*, 2023). MWT (rotor diameter (D)  $\leq$  12.5 m) could be one of the sustainable options (Gipe, 2009). This can be achieved by optimizing the energy production generated from the MWT at low wind speeds and different wind directions (Ozgener, 2006). Hence, it must be designed and reinforced to work effectively under different weather conditions. MWT can be classified into horizontal and vertical wind turbines like conventional wind turbines. According to Betz's law, 59.26% of the kinetic energy in the wind could be converted to mechanical energy by a wind turbine. In contrast, this percentage decreased to 14.8% in MWTs. MWTs can be installed on any building roof, operate at low airspeeds, and have little impact on the surrounding ecosystem (Peacock *et al.*, 2008). They also require little or no maintenance and have a longer life compared to standard turbines. However, the power production of MWTs is limited to applications with low wind speeds and is lower compared to traditional wind turbines (Aljafari *et al.*, 2022; Tummala *et al.*, 2016; Wilberforce *et al.*, 2023). Large-scale wind turbines encountered significant challenges. One of these challenges is changing the wind direction over a short period (Chang *et al.*, 2022). This challenge is particularly pronounced in southern Jordan, where many wind turbine farms have been established. MWT can overcome this challenge by harvesting energy from the wind at an angle of about 300. In addition, it can work if it faces the wind from both sides (it works as an upwind and downwind turbine). However, the best performance is when the wind is perpendicular to the MWT blades. Thus, in this work, the MWT has been reconstructed based on previous investigations conducted by Leung *et al.* (Leung *et al.*, 2010) and studies at Hong Kong University and Lucien Gamba Rota of Motorwave Ltd. The structure of the MWT has been tested numerically in the SolidWorks environment. Different torque values have been applied to investigate its ability to work under various conditions. Then, the MWT structure has been thermally tested over different working temperatures. CFD model was created using ANSYS- Fluent to investigate the turbine performance. This model has been validated experimentally by testing MWT in the wind tunnel, and an assessment has been conducted on the manufacturing techniques presently accessible for micro-wind turbines. The contribution of this paper is to study MWT using the available tools to make it more durable, reliable, and able to withstand different weather conditions.

## 2. Method

### 2.1. Experimental Work

The MWT design has been reconstructed based on the recommendations of Leung *et al.* (Leung *et al.*, 2010). The MWT has 5 fan-shaped blades with a twist angle of approximately 31° and a radius of 117 mm, as shown in Fig.1. Table 1 summarizes the properties of the MWT's. The structure of this turbine was built by Poly Lactic Acid (PLA) filament using 3D printing techniques. This material is a widely used in 3D printing due to its many properties, like low melting point, high strength, low thermal expansion, etc. (Raj *et al.*, 2018). Table 2 summarizes the properties of PLA material (Fernandes *et al.*, 2018). Model experiments in wind tunnels under idealized and controlled environmental conditions are crucial in developing wind turbines. The investigation was conducted in a wind tunnel in the AL-Hussein Bin Talal University (AHU) laboratory in Ma'an, Jordan. The primary objective of this test was to validate the MWT numerical model and observe the device response when subjected to constant airspeed conditions. So, an open circuit wind tunnel (GUNT, model HM 170) has been utilized to test such models produced by 3D printing from PLA material. The experiment was conducted under an ambient temperature ( $T_{atm}$ ) of about 20 °C and atmospheric pressure ( $P_{atm}$ ) of 1013 hPa. The axial fan on the right side of the wind tunnel, as shown in Fig.2 can generate constant airspeed from 3.1 to 28 m/s and a pressure differential of 500 Pa. An inclined tube manometer can measure the airspeed value in the measuring section. The flow cross-section has a dimension of 292 mm wide, 292 mm high and a length of about 420 mm. For increased measurement accuracy, an anemometer (model-DT-73G, accuracy  $\pm 3\%$   $\pm 0.20$  m/s) also has been used to measure the airspeed besides a wind tunnel's inclined tube manometer. A digital tachometer (model-ET2320, accuracy  $\pm 0.05\%$  1- digits) has been used to measure the rotational speed of the MWT (RPM).

MWT has been mounted in the section of the test chamber (see Fig.2). The test can be started by running the axial fan to allow air to suck in from the atmosphere through a straightener that provides uniform airspeed distribution with little turbulence. The airflow has been accelerated up to 4 m/s (Reynolds Number,  $Re=1.12 \times 10^8$ ) in the nozzle and flowed around the MWT in the measuring section. Then, the diffuser reduced airspeed before it was pumped into the open air by the axial fan. Under this condition, the MWT was rotate 445 RPM. The characteristics of wind turbines can be studied by representing the relationship between power coefficient ( $C_p$ ) torque (T) with Tip Speed Ratio (TSR). The power coefficient ( $C_p$ ) can be defined as the power produced by the wind turbine with total power available in the wind which can be defined as:

**Table 1**  
MWT characteristics

Characteristics	Value
Chamber to chord ratio	6%
Blade thickness	1.5 mm
Blade shape	Fan type blade
Angle of twist	31°
Subtend angle	60°
Solidity	65%
Reynolds number	38433
Turbine radius	117 mm

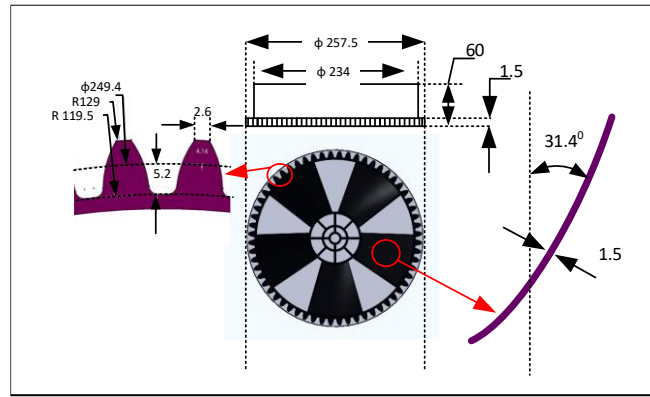


Fig. 1 Geometry of MWT in (mm)

Table 2  
Properties of PLA material

Property	Value
Density	1.26 g/cm <sup>3</sup>
Tensile yield	49.5 MPa
Tensile modulus	2346.5 MPa
Strain at yield point	3.3%
Bending stress	103 MPa
Poisson ration	0.36
Shear strength	33 MPa
Shear modulus	2400 MPa
Compressive strength	93.76 MPa
Surface roughness	2.46µm - 22.48 µm

$$C_p = \frac{P_R}{TSR \times P_w} \tag{1}$$

$$P_R = T \omega \tag{3}$$

where the total power in wind flowing through swept area (A) can be calculated from Eq.(2) :

$$P_w = \frac{1}{2} \rho V_a^3 A \tag{2}$$

The TSR can be defined as the ration between the speed of the rotor to the wind speed, as given in Eq.(4),

$$TSR = \frac{\omega \times r}{V_a} \tag{4}$$

The rotor power (P<sub>R</sub>) is the rotor power as product torque (T) and rotational speed (ω) of turbine can be defined as:

2.2. Numerical Model

The initial phase of this study involved developing a 3D model of the MWT using SolidWorks 2019 software, based on the geometry shown in Fig. 1. The SolidWorks Flow Simulation

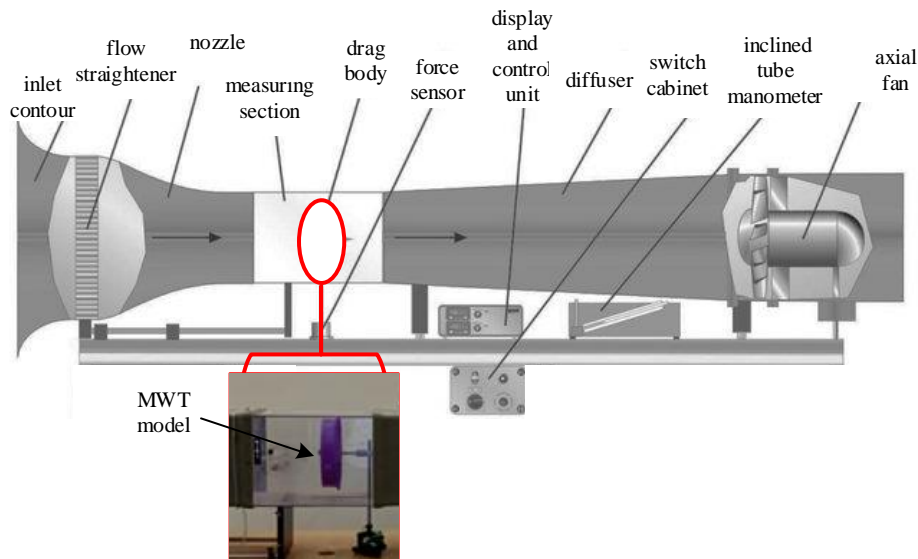


Fig. 2 Experimental setup of the MWT

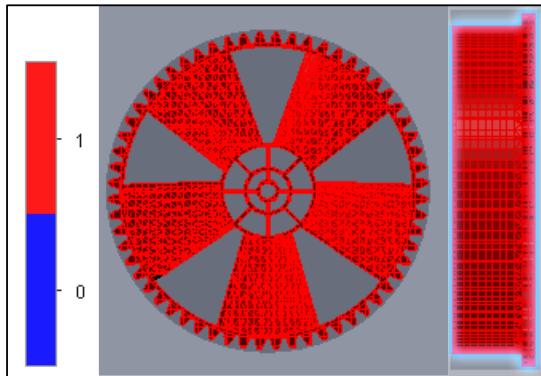


Fig. 3 The computational domain of the structural analysis.

(SFS) tool was employed to perform stress-strain and thermal analysis to ensure that the turbine would function effectively in the expected weather conditions at the installation site. Subsequently, the computational Fluid dynamics (CFD) method was utilized to assess the performance of the MWT, utilizing the Fluid Flow (Fluent) software provided by ANSYS.

2.2.1. Structural and thermal analysis

During MWT operation, the vibration that occurs at different operating speeds, hot or cold weather temperatures and other operational factors affect the longevity of the MWT blade. Thus, the mechanical properties of a material, such as its strength, stiffness, and ductility or MWT, should be determined (Lanzotti et al., 2015). In this work, structural analysis has been conducted according to the ASTM D-638 standard by SolidWorks software to determine the behaviour of MWT material under service conditions. In addition, the thermal stress aspects have been analysed to investigate whether the PLA material can withstand stress and torque at various temperatures. The dynamic elasticity modulus has been considered in a SolidWorks environment. The 3D model of the turbine was drawn by 3D CAD design software (SolidWorks), and the properties of the Poly Lactic Acid (PLA) material was defined. Then, the computational domain was created for the turbine, as shown in Fig.3. This domain consists of  $1.902 \times 10^6$  elements. It has  $0.882 \times 10^6$  solids elements with red color (No.1) and  $1.02 \times 10^6$  elements with blue color (No.2) of the fluid surrounding the turbine.

2.2.2. Computational fluid dynamics (CFD)

The performance of MWT could be evaluated using computational fluid dynamics (CFD) (Abrar et al., 2014; White & Wakes, 2014). Thus, to do more investigation on the MWT, Computational Fluid Dynamics (CFD) was utilized in this work. The analysis was performed using Fluid Flow (Fluent) provided by ANSYS. This software applies the continuity equation Eq. (5) and momentum equation Eq. (6) of the Navier–Stokes equations (NS) to describe the incompressible fluid flow motion (ANSYS-Fluent, 2009). A simulation study on an MWT using ANSYS Fluent Fluid Simulation software is one of the feasible techniques used to study the main parameters used in the turbine design like blade thickness and the best shape of the blades, the number of blades, blade chamber, angle of twist, subtend angle, turbine radius, blade tapering, and solidity. Favre-averaged Navier-Stokes equations are used to predict turbulent flows. ANSYS Fluent employs transport equations for the turbulent kinetic energy and its dissipation rate using the k-ε model to close this system of equations (Matsson, 2022).

$$\nabla \cdot \bar{u} = 0 \tag{5}$$

$$\rho \left( \frac{\partial \bar{u}}{\partial t} + \bar{u} \nabla \bar{u} \right) = -\nabla \bar{p} + \bar{u} \nabla^2 \bar{u} + \rho \cdot g_i - \rho \frac{\partial \tau_{ij}}{\partial \chi_i} \tag{6}$$

where  $i, j = 1, 2, 3$  for three-dimensional flows

Since the fluid flow was located outside the geometry, the transient analysis has been specified in this model. Also, fresh air was chosen as the operating fluid in the pre-processor. Then, the k-ε model was selected as the turbulence model as it was suitable for identifying the effects on a surface (Menter, 1994). Finally, airspeed was adjusted at  $V_a = 4 \text{ m/s}$  in the initial run. The computational domain was then positioned, i.e., inlet, turbine, blade angle, and outlet. The computational domain border was defined, as shown in Fig. 4. The domain (in mm) was  $x=0.359, y= 0.359$  and  $z= 0.512$ . This is to resolve the pressure and velocity concerns at each part of the domain. The accuracy of the calculations is related to the mesh, where the network has been sufficiently condensed in the turbine model (tetrahedrons cell has been chosen) to produce accurate results with the lowest possible computational cost (ANSYS-Fluent, 2009). Fig. 5 illustrated meshing display of turbine by Cartesian meshing. The boundary conditions used for the CFD model are given in Table 3. The specific grid of a turbine - CFD consists of  $1.902 \times 10^6$  elements,  $0.5106 \times 10^6$  elements of solids and  $1.02 \times 10^6$  elements of the fluid surrounding the turbine. The number of iterations specified in the solvent is 20000-time steps, each time step is 0.000025 seconds long and 5-iterations for each time step to achieve converged.

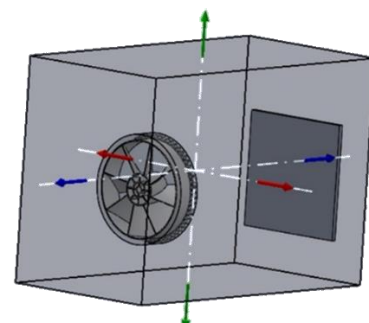


Fig. 4 Computational fluid domains

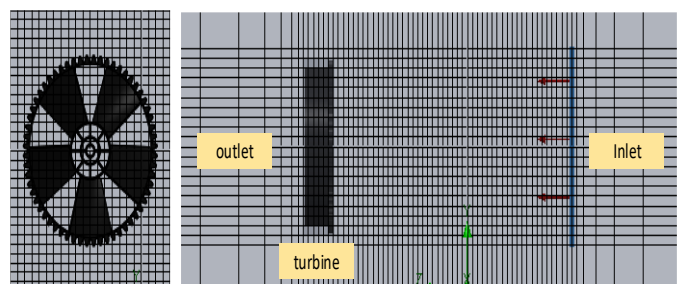
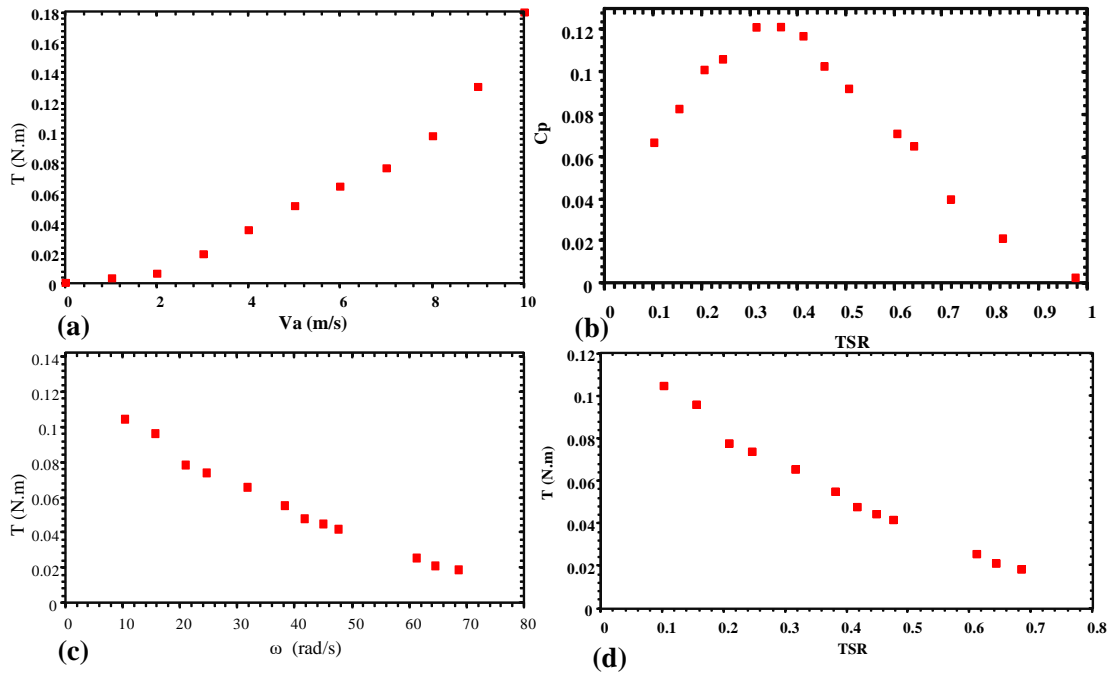


Fig. 5 Meshing geometry of the MWT

Table 3  
CFD Boundary conditions

Inlet	Enclosure	MWT	Wall	Outlet
airspeed 3.77 m/s	No slip	No slip	Specified Shear	Pressure outlet



**Fig. 6** Experimental characteristics of MWT.(a) Effect of airspeeds  $V_a$  (m/s) variations on the torque T (N.m), (b) The effect of TSR on Power Coefficient ( $C_p$ ) at a constant airspeed of 4 m/s,(c) Effect of angular velocity  $\omega$  (rad/s) variations on the torque T (N.m), and (d) The effect of TSR on the torque T (N.m)

### 3. Results and Discussion

#### 3.1. Experimentally evaluate the MWT performance

The experiments were conducted in a wind tunnel under controlled environmental conditions to validate the numerical

models and observe the device response when subjected to constant airspeed conditions. The performance parameters, including the power coefficient ( $C_p$ ), tip speed ratio (TSR), and angular velocity, were examined to evaluate the efficiency and effectiveness of the MWT design. In Fig. 6, the characteristics of the MWT are represented, and it is clearly shown in Fig.6-(a)

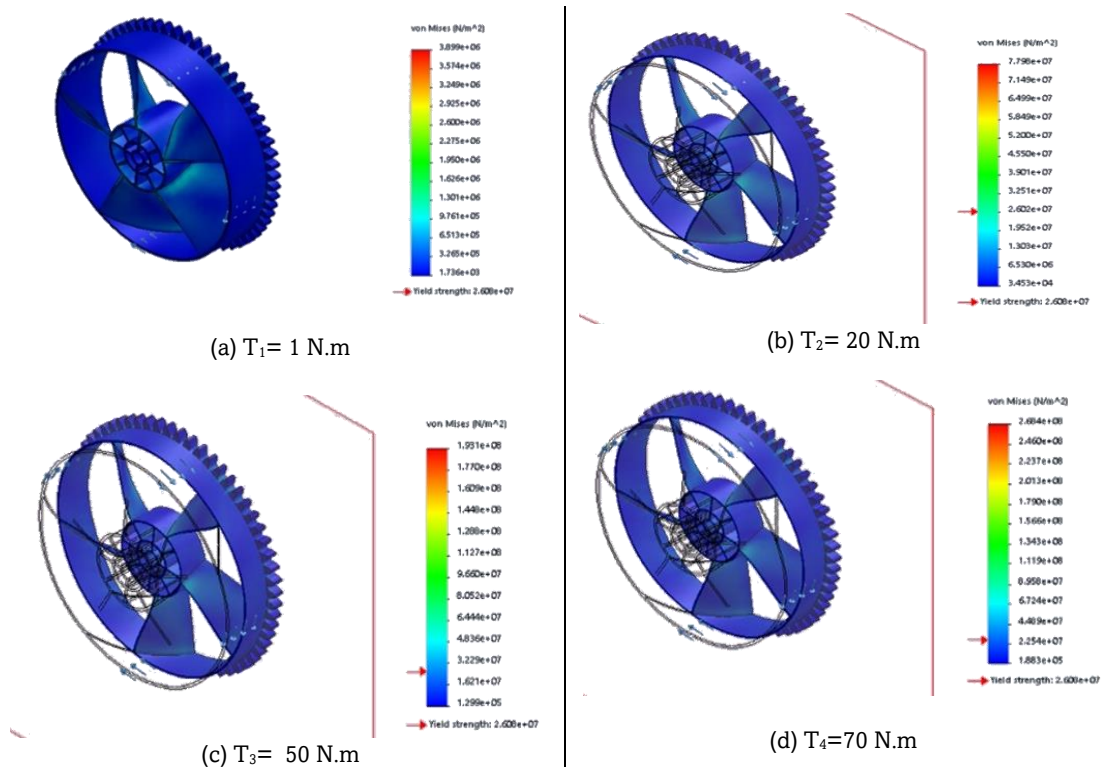


**Fig. 7** MWT test under torques (a)  $T=1 \text{ N.m}$ , (b)  $T=20 \text{ N.m}$ , (c)  $T= 50 \text{ N.m}$  and (d)  $T= 80 \text{ N.m}$ .

that the torque becomes valuable after airspeed is higher than 2 m/s. The start-up wind speed is relatively low, which meets the design intent of this type of wind turbine. The relationship between the power coefficient and TSR has been obtained based on Eq. (1), as shown in Fig. 6-(b). The power coefficient ( $C_p$ ) increased with increasing TSR reaching its maximum at the optimal TSR and then decreasing thereafter. As indicated in Fig. 6-(b), the tip speed ratio of the present MWT is between 0 and 0.95, which meets closely with the traditional, small, multi-bladed wind turbine. Besides, the MWT maximal power coefficient indicates that the  $C_p$  is about 0.12%. Figs. 6-(c) and 6-(d) show the torque (T) curve versus angular velocity and TSR for MWT, respectively. These two figures have the same pattern; the torque decrease with an increase  $\omega$  and TSR. The torque at low TSR values has maximum values and decreases with TSR.

3.2. Structural and thermal analysis results

Using PLA material in 3D printing is a promising technique. It is increasingly being used for the development of smart textiles. However, under certain levels of twisting or rotational forces, PLA can exhibit plastic deformation, affecting the integrity and durability of 3D-printed objects. Accordingly, structural, and thermal analysis has been conducted on SolidWorks software to provide valuable insights into the design and performance of the 3D-printed MWT, which can inform future improvements and optimizations. The MWT has been tested under several torque values to reach the failure point. The PLA material response under different twisting or rotational force levels was presented in Figs.7 (a-d). Under low torques ( $T=1$  N.m and  $T=20$  N.m, Figs.7(a) (b)), the PLA experienced

relatively low levels of stress and strain. In contrast, the stress and strain become the worst impact under increasing the torque applied ( $T=50$  N.m and  $T=70$  N.m, Figs.7(a) (b)). This relation is represented clearly in Fig.8. This figure indicates that the material exhibited a linear stress-strain response, with a small increase in strain corresponding to a small increase in stress. When high torques were applied ( $>50$  N.m.), the PLA experienced elevated levels of stress and strain ( $>200$  N.m<sup>2</sup>,  $>25$ , respectively). The PLA material failed by applying a torque of more than 70 N.m. Thus, the maximum torque value for the MWT should be less than 70 N.m.

LA is generally considered a Non-Newtonian fluid; while it may exhibit Newtonian behavior under certain conditions, such as at low shear rates or temperatures, it can also behave as a pseudoplastic or thixotropic fluid under other conditions (Hamad *et al.*, 2011). As shown in Fig.9, at low temperatures (25 °C, 30 °C), the mechanical properties of PLA tend to be improved as the material becomes stiffer and stronger. This is due to the decrease in molecular mobility and reduced material viscosity at low temperatures. In contrast, at high temperatures (40 °C and 50 °C), the mechanical properties of PLA tend to degrade as the material becomes softer and less stiff. This is due to the increase in molecular mobility and increased viscosity of the material at high temperatures, which reduces its ability to withstand stress and strain.

3.3. Validation of the CFD model

One of the aims of this work is to validate the CFD model with physical experiments of MWT. The main MWT characteristics, like the  $C_p$ , TSR and the relation of torque with angular velocity, were compared for CFD validation, as shown in Fig.10. The agreement between the experiment and numerical results was quantified via the Normalized Root Mean Square Error (NRMSE). The effect of airspeed  $V_a$  (m/s) variations on the angular velocity  $\omega$  (rad/s) was analysed and compared to the experimental data. The results are presented in Fig.10-(a), which shows a good agreement between the CFD predictions and the experimental data with correlation coefficient R about 0.98 and NRMSE about 5.4%. The impact of TSR on the Power Coefficient ( $C_p$ ) was studied at a constant airspeed of 4 m/s. The comparison between the CFD model and experimental data is presented in Fig.10-(b), which shows a reasonable agreement between the two with correlation coefficient R about 0.95 and an average NRMSE of 10.5%. The effect of angular velocity  $\omega$  (rad/s) variations on the torque T (N.m) was investigated and compared to experimental data. Fig.10-(c) presents the comparison between the CFD model and experimental data, which shows good agreement with correlation coefficient R about 0.98 and an average NRMSE of 21.1%. The average NRMSE for the characterizes was 12.33%, which was deemed acceptable.

This investigation's numerical and experimental results aligned with the MWT designed by Leung *et al.* (Leung *et al.*, 2010). The optimal TSR of the 5-bladed MWT was found to range from 0.5 to 0.6 in previous work, resulting in a power coefficient of slightly above 0.1. The current work's optimal TSR range was from 0.4 to 0.5, with a power coefficient of approximately 0.12. This difference in results is likely due to variations in the experimental conditions. Furthermore, the starting effect (torque) under different wind speeds is comparable between this work and the previous work by Leung *et al.* (Leung *et al.*, 2010).

Once the numerical model was validated, the validated CFD model was employed to compare a 5-bladed with a 60-degree blade and 8- bladed and estimated the performance of such MWT. Fig.11 shows the velocity contours around the

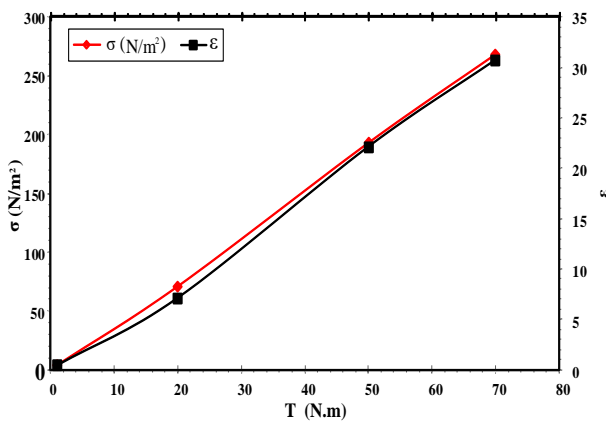


Fig. 8 The changes in MWT stress-strain under different torque.

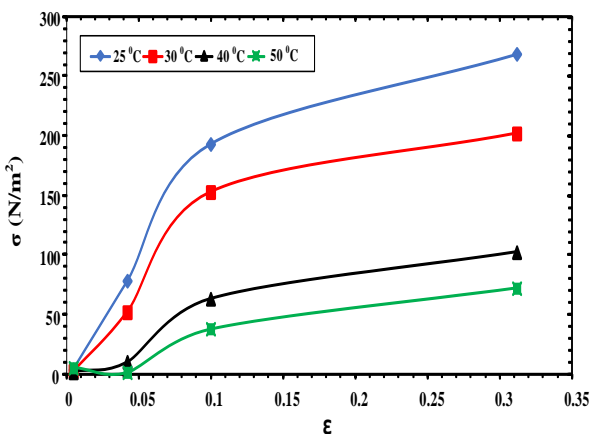
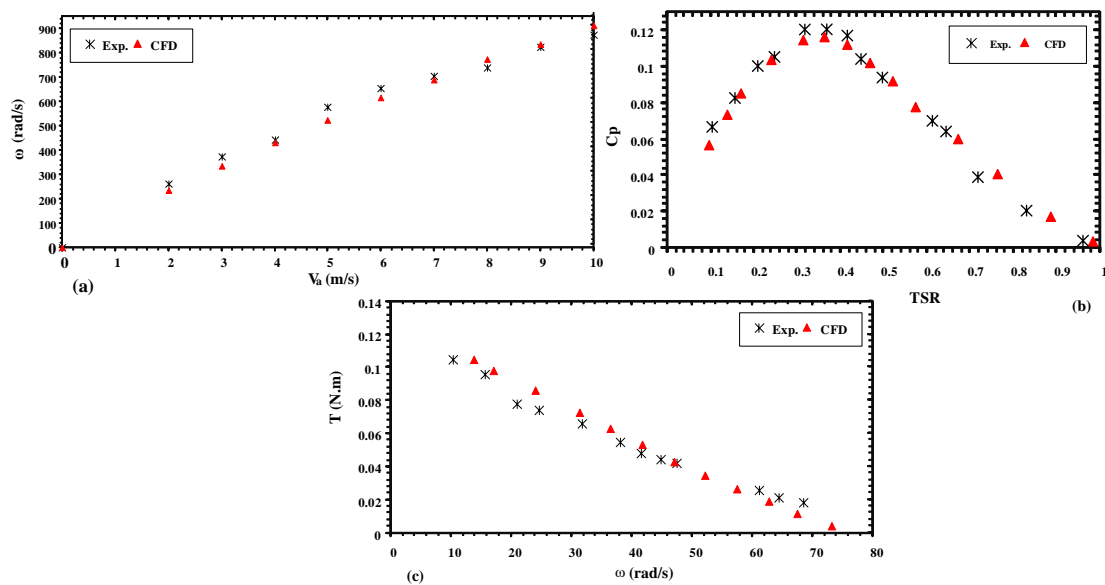
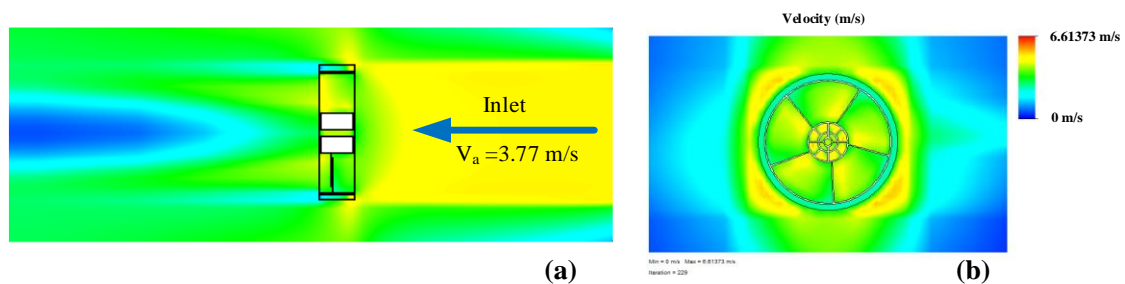


Fig. 9 The changes in MWT stress-strain under different operating temperatures



**Fig. 10** Comparison of experimental and CFD results for MWT characteristics. (a) The effect of airspeed  $V_a$  (m/s) variations on the angular velocity  $\omega$  (rad/s), (b) The impact of TSR on Power Coefficient ( $C_p$ ) at a constant airspeed of 4 m/s and (c) The effect of angular velocity  $\omega$  (rad/s) variations on the torque  $T$  (N.m).



**Fig. 11** Velocity contours of (a) yz plane (b) xz plane

MWT obtained from the CFD simulation. According to Fig.11-(a), the inlet airspeed of 3.77 m/s. The incoming wind speed decreases from 3.77 m/s to about 2.53-2.06 m/s directly behind the blade (about a 32.89% - 45.36 decrease). While the flow remains at the same inlet velocity between the blade and around the turbine, as shown in Fig.11-(b). The indication of successful energy transfer can be visualized by observing the velocity counter before and after the turbine.

As Leung, Deng, and Leung recommended (Leung *et al.*, 2010), the optimal turbine profile is the 5-bladed with a 60-degree blade subtend angle. However, a comparison between a 5-bladed MWT with a 60-degree blade and an 8-bladed MWT was conducted using a CFD model, as shown in Fig.12. It was found that the 8-bladed MWT can operate under high torque with a cut-in speed of 3.77 m/s, which is higher than the cut-in speed of the 5-blade MWT (2.01 m/s). On the other hand, the 5-blade MWT can work only under low torque values. Although, A high start-up torque at low wind speeds will enhance energy harnesses (Selig, 1997). Therefore, if multiple MWTs operate simultaneously, the 8-blade configuration is recommended. However, a 5-blade configuration was chosen for the present study to capture more power at low wind speeds. The influence of blade angle variation on torque was numerically examined, as shown in Fig. 13.

The results indicate that the MWT generates more torque with a 31-degree blade angle compared to other angles, which led to the selection of this angle for manufacturing, as illustrated in Fig. 1. The power generated by the MWT at various wind speeds has been analyzed by utilizing the power curve data

displayed in Fig.14. At a wind speed of 4 m/s, the power output is around 0.4 W. The MWT is capable of generating more power at low wind speeds compared to other turbines, such as the two MWT prototypes examined by (Akour *et al.*, 2018), given its size.

### 3.4. Economic Considerations

Injection molding and 3D printing are two manufacturing methods that can produce MWTs in the Jordan market. Polypropylene (PP) plastic can be used in the injection molding process, a versatile and economical material used in various industries, including military, automobile, and aerospace. The total weight of the proposed MWT is 0.352 kg, and it is estimated that 2830 turbines can be produced from 1 ton of polypropylene, assuming 10% of the material is wasted. The cost of making one MWT is approximately 0.25 JD (0.35 \$), based on producing 2830 pieces. The estimated cost of 1 ton of polypropylene in the Jordan local market is 1200-1300 JD (1691.83\$-1832.82 \$), so the raw material cost for one MWT is about 0.46 JD (0.65\$). Injection molding of 1 ton of polypropylene consumes 5600 kW.h. The electricity cost follows the following pricing structure in Jordan: 50 fils per kilowatt-hour for 1-300 kilowatt-hours, 100 fils per kilowatt-hour for 301-600 kilowatt-hours, and 200 fils per kilowatt-hour for more than 600 kilowatt-hours, resulting in an energy cost of approximately 0.37 JD (0.52 \$) per MWT. Finally, each MWT requires a surface finish to smooth the blades, with an estimated cost of 0.5 JD (0.70\$) based on the average labor salaries in Jordan in 2023. The total cost of producing one MWT is

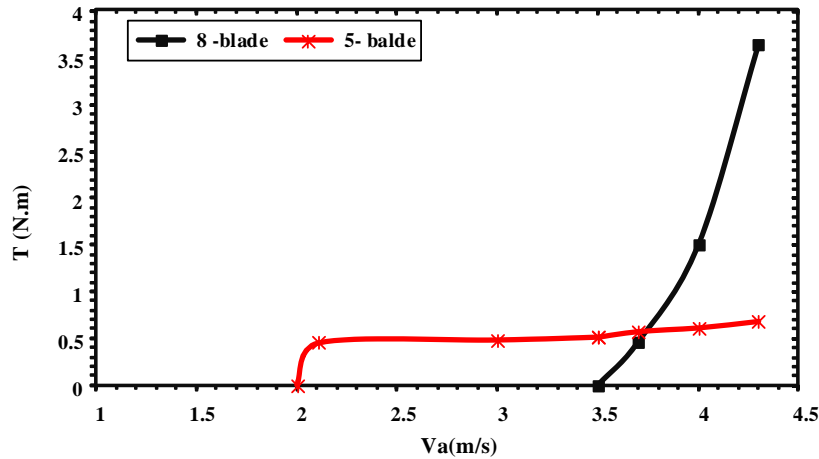


Fig. 12 The numerical difference between 5-blades and 8-blades

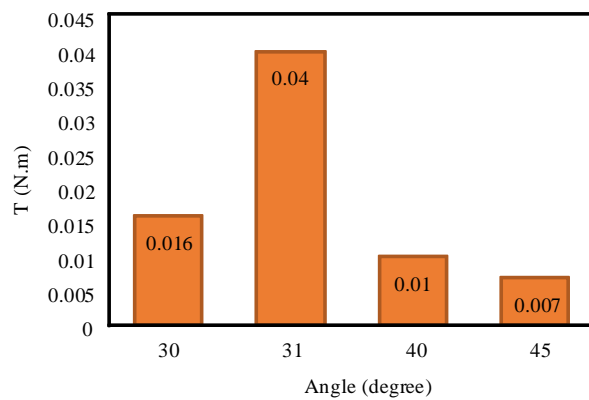


Fig. 13 The numerical values of torque at different blade angles of MWT (5- blades model).

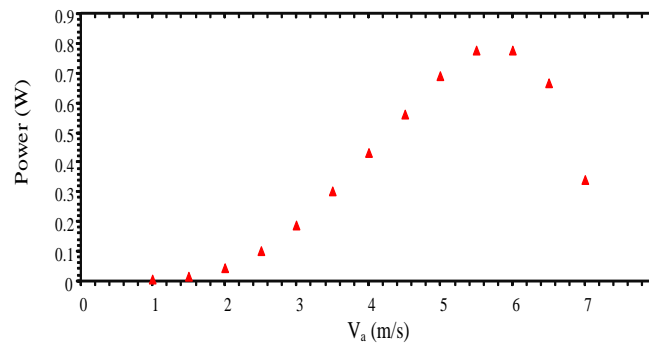


Fig. 14 The power curves of the MWT under different wind speed

Table 4

Total costs of one MWT produced

Cost type	Price (JD)	
	Injection molding	3D printing method
Production	0.25	0
Material	0.46	7.0
Manufacturing	0.52	23
Surface finish	0.50	1.0
<b>Total</b>	<b>1.73</b>	<b>31</b>

summarized in Table 4 and is estimated to be about 1.73 JD (2.44\$).

In the 3D printing method, the material used in the manufacture is polylactide (PLA). It is the most widely used

material for 3D printing and is characterized by its low melting point, high strength, low thermal expansion, good adhesion to the layer and high heat resistance when annealing. The cost of using a 3D printer to carry out manufacturing, including operations and consumed electricity, is estimated at 0.464 JD per working hour. For such MWT, the printer needs 49 hours to complete the project's work. Thus, each MWT costs about 23 JD (32.43\$). 20.0 JD/ kg is the price of PLA material in the local market. Thus according to the estimated weight of the MWT model (0.352 kg), each MWT costs approximately 7 JD for a PLA material. Finally, each MWT needs a surface finish to make the blade smoothie. The cost of doing that is about 1.0 JD (1.40 \$), according to the average labor salaries in Jordan in 2023. Accordingly, the total cost of preparing one piece of MWT by a 3D printer is about 31 JD (43.71\$), as summarized in Table 4.

Injection molding is characterized by high accuracy and a fine surface finish for the MWT blades. In contrast, the 3D

printer requires additional surface finishing to improve its accuracy, and the precision of the finished product is lower compared to injection molding. This cost of production may decrease once the turbines are mass-produced using injection molding. However, in this work, a 3D printing method has been used due to the high initial cost of molds. In Jordan, the average power consumption per capita is an average of 1,509 kWh. The one-year average wind speed in Jordan is about 3.5 m/s. The single MWT is designed to provide 16 Wh/day if the MWT operates for 16 hours. This value of power generated can be increased at larger wind speeds. However, a more significant amount of useful power can be obtained by grouping several of these MWTs for power generation. A target site for deploying the MWT will be on the rooftop of residential buildings with heights of up to 10 m. The estimated MWTs required for a particular site are unavailable in this research stage. It will be calculated based on the available wind power and average power produced in future work.

#### 4. Conclusion

Micro-wind turbines (MWTs) have the potential to provide electricity for residential and remote consumers in areas with sufficient wind resources. In this study, a 5-blade MWT was reconstructed using 3D printing techniques and tested numerically and experimentally. The 5-blade design was found to be more effective than an 8-blade design, with a lower cut-in speed and less torque. The mechanical behavior of the MWT material was studied under different operating temperatures. It was found that PLA material could be used efficiently to produce an MWT with a low deformation rate and less stress and strain during load. Accordingly, the weather conditions in southern Jordan will be appropriate for operating this type of turbine. The MWT underwent wind tunnel tests to verify the CFD model, and the two models were found to be an acceptable match, with an NRMSE of about 1.1%. The operating TSR of the MWT was found to range from 0.1 to 0.85, which measures the effectiveness of wind turbine blades in converting wind energy to rotational energy. The study suggests that MWTs could play a significant role in future energy production due to their installation, monitoring, and maintenance simplicity. Further research should evaluate the performance of multiple MWTs under realistic conditions to determine energy production and efficiency.

#### Reference

Abrar, M. A., Mahub, A. I., & Mamun, M. (2014). Design optimization of a horizontal axis micro wind turbine through development of CFD model and experimentation. *Procedia Engineering*, *90*, 333-338. <https://doi.org/10.1016/j.proeng.2014.11.858>

Ajadi, T., Cuming, V., Boyle, R., Strahan, D., Kimmel, M., Logan, M., & McCrone, A. (2020). Global Trends in Renewable Energy Investment 2020. [https://www.fs-unep-centre.org/wp-content/uploads/2020/06/GTR\\_2020.pdf](https://www.fs-unep-centre.org/wp-content/uploads/2020/06/GTR_2020.pdf)

Akour, S. N., Al-Heydari, M., Ahmed, T., & Khalil, K. A. (2018). Experimental and theoretical investigation of micro wind turbine for low wind speed regions. *Renewable energy*, *116*, 215-223. <https://doi.org/10.1016/j.renene.2017.09.076>

Aljafari, B., Samithas, D., Balachandran, P. K., Anandan, S., & Babu, T. S. (2022). Performance Analysis of PLA Material Based Micro-Turbines for Low Wind Speed Applications. *Polymers*, *14*(19), 4180. <https://doi.org/10.3390/polym14194180>

ANSYS-Fluent. (2009). *ANSYS FLUENT 12.0* (Theory Guide), ANSYS, Issue.

Aravindhan, N., Natarajan, M., Ponnuvel, S., & Devan, P. (2022). Recent developments and issues of small-scale wind turbines in urban

residential buildings-A review. *Energy Environment*. Online first, <https://doi.org/10.1177/0958305X221084038>

Ayhan, D., & Saglam, S. (2012). A technical review of building-mounted wind power systems and a sample simulation model. *Renewable Sustainable Energy Reviews*, *16*(1), 1040-1049. <https://doi.org/10.1016/j.rser.2011.09.028>

Bangi, V.K.T., Chaudhary, Y., Guduru, R.K., Aung, K.Tand Reddy, G.N. (2017) Preliminary investigation on generation of electricity using micro wind turbines placed on a car. *Int. Journal of Renewable Energy Development*, *6*(1), 75-81. <https://doi.org/10.14710/ijred.6.1.75-81>

Carré, A., Roux, É., Tabourot, L., & Gasnier, P. (2022). Innovative blade shape for micro wind turbines. 2022 Wireless Power Week (WPW), <https://doi.org/10.1109/WPW54272.2022.9854036>

Chang, C. C. W., Ding, T. J., Ping, T. J., Chao, K. C., & Bhuiyan, M. A. S. (2022). Getting more from the wind: Recent advancements and challenges in generators development for wind turbines. *Sustainable Energy Technologies Assessments*, *53*, 102731. <https://doi.org/10.1016/j.seta.2022.102731>

Chaudhuri, A., Datta, R., Kumar, M. P., Davim, J. P., & Pramanik, S. (2022). Energy conversion strategies for wind energy system: Electrical, mechanical and material aspects. *Materials*, *15*(3), 1232. <https://doi.org/10.3390/ma15031232>

Chudzick, S. (2023). Wind Microturbine with Adjustable Blade Pitch Angle. *Energies*, *16*(2), 945. <https://doi.org/10.3390/en16020945>

Clausen, P., & Wood, D. (2000). Recent advances in small wind turbine technology. *Wind Engineering*, *24*(3), 189-201. <https://doi.org/10.1260/0309524001495558>

Council, G. W. E. (2021). *GWEC Global Wind Report 2021*. <https://www.gwec.net/global-wind-report-2021/>

Diógenes, J. R. F., Claro, J., Rodrigues, J. C., & Loureiro, M. V. (2020). Barriers to onshore wind energy implementation: A systematic review. *Energy Research Social Science*, *60*, 101337. <https://doi.org/10.1016/j.erss.2019.101337>

Fernandes, J., Deus, A. M., Reis, L., Vaz, M. F., & Leite, M. (2018). Study of the influence of 3D printing parameters on the mechanical properties of PLA. *Proceedings of the 3rd International Conference on Progress in Additive Manufacturing* (Pro-AM 2018), Singapore, <https://dr.ntu.edu.sg/handle/10220/45960>

Gipe, P. (2009). *Wind energy basics: a guide to home and community-scale wind-energy systems*. Chelsea Green Publishing.

Gordon, M., Weber, M., & Raj, P. (2021). Global energy demand to grow 47% by 2050, with oil still top source: *US eia* Retrieved 10.03.2023 from <https://www.spglobal.com/platts/en/market-insights/latest-news/oil/100621-global-energy-demand-to-grow-47-by-2050-with-oil-still-top-source-us-eia>

Hamad, K., Kaseem, M., & Deri, F. (2011). Melt rheology of poly (lactic acid)/low density polyethylene polymer blends. *Advances in Chemical Engineering Science*, *1*(4), 208-214. <http://www.10.4236/aces.2011.14030>

IRENA. (2022). *World Energy Transitions Outlook 2022: 1.5°C Pathway*. International Renewable Energy Agency, Abu Dhabi; y, Abu Dhabi. <https://www.irena.org/publications>

Kumar, N., & Prakash, O. (2023). Analysis of wind energy resources from high rise building for micro wind turbine: A review. *Wind Engineering*, *47*(1), 190-219. <https://doi.org/10.1177/0309524X221118684>

Lakatos, L., Hevessy, G., & Kovács, J. (2011). Advantages and disadvantages of solar energy and wind-power utilization. *World Futures*, *67*(6), 395-408. <https://doi.org/10.1080/02604020903021776>

Lanzotti, A., Grasso, M., Staiano, G., & Martorelli, M. (2015). The impact of process parameters on mechanical properties of parts fabricated in PLA with an open-source 3-D printer. *Rapid Prototyping Journal*, *21*(5), 604-617; <https://doi.org/10.1108/RPJ-09-2014-0135>

Leung, D., Deng, Y., & Leung, M. (2010). Design optimization of a cost-effective micro wind turbine. *Proceedings of the World Congress on Engineering*,

Li, G., Li, M., Taylor, R., Hao, Y., Besagni, G., & Markides, C. (2022). Solar energy utilisation: Current status and roll-out potential. *Applied Thermal Engineering*, *209*, 118285. <https://doi.org/10.1016/j.applthermaleng.2022.118285>

Matsson, J. E. (2022). *An Introduction to ANSYS Fluent 2022*. Sdc Publications.

- Menter, F. R. (1994). Two-equation eddy-viscosity turbulence models for engineering applications. *AIAA journal*, 32(8), 1598-1605. <https://doi.org/10.2514/3.12149>
- Naqash, M. T., Aburamadan, M. H., Harireche, O., AlKassem, A., & Farooq, Q. U. (2021). The Potential of Wind Energy and Design Implications on Wind Farms in Saudi Arabia. *International Journal of Renewable Energy Development*, 10(4), 839-856. <https://doi.org/10.14710/ijred.2021.38238>
- Nijssen, R., & Brøndsted, P. (2023). Fatigue as a design driver for composite wind turbine blades. In *Advances in wind turbine blade design and materials* (pp. 217-248). Elsevier. <https://doi.org/10.1016/B978-0-08-103007-3.00006-9>
- Ozgener, O. (2006). A small wind turbine system (SWTS) application and its performance analysis. *Energy conversion management*, 47(11-12), 1326-1337. <https://doi.org/10.1016/j.enconman.2005.08.014>
- Peacock, A., Jenkins, D., Ahadzi, M., Berry, A., & Turan, S. (2008). Micro wind turbines in the UK domestic sector. *Energy buildings*, 40(7), 1324-1333. <https://doi.org/10.1016/j.enbuild.2007.12.004>
- Raj, S. A., Muthukumaran, E., & Jayakrishna, K. (2018). A case study of 3D printed PLA and its mechanical properties. *Materials Today: Proceedings*, 5(5), 11219-11226. <https://doi.org/10.1016/j.matpr.2018.01.146>
- Rao, K. (2019). Wind energy for power generation: meeting the challenge of practical implementation. Springer Nature. ISSN: 978-3-319-75134-4; <https://doi.org/10.1007/978-3-319-75134-4>
- Raut, S., Shrivastava, S., Sanas, R., Sinnarkar, N., & Chaudhary, M. (2017). Simulation of micro wind turbine blade in Q-Blade. *J. Res. Appl. Sci. Eng. Technol*, 5(4), 256-262. <https://doi.org/10.22214/ijraset.2017.4048>
- Razzetti, D. (2022). Aerodynamic design of a micro wind turbine and performance analysis with QBlade. Thesis. Politecnico di Torino. <http://webthesis.biblio.polito.it/id/eprint/22493>
- Rehman, A., Alam, M. M., Ozturk, I., Alvarado, R., Murshed, M., Işık, C., & Ma, H. (2023). Globalization and renewable energy use: how are they contributing to upsurge the CO2 emissions? A global perspective. *Environmental Science Pollution Research*, 30(4), 9699-9712. <https://doi.org/10.1007/s11356-022-22775-6>
- Roga, S., Bardhan, S., Kumar, Y., & Dubey, S. K. J. (2022). Recent technology and challenges of wind energy generation: A review. *Sustainable Energy Technologies Assessments*, 52, 102239. <https://doi.org/10.1016/j.seta.2022.102239>
- Scarabaggio, P., Grammatico, S., Carli, R., & Dotoli, M. (2021). Distributed demand side management with stochastic wind power forecasting. *IEEE Transactions on Control Systems Technology*, 30(1), 97-112. <https://doi.org/10.1109/TCST.2021.3056751>
- Selig, M. S. (1997). *Summary of low speed airfoil data Vol. 3*. SoarTech Publications.
- Spera David, A. (1995). *Wind Turbine Technology, 3rd ed.* ASME Press.
- Sun, H., Dang, Y., Mao, W., & Luo, D. (2021). Optimal path for overcoming barriers in developing China's wind energy industry. *Environmental Science Pollution Research*, 28(27), 35597-35612. <https://doi.org/10.1007/s11356-021-12531-7>
- Tan, J. D., Chang, C. C. W., Bhuiyan, M. A. S., Nisa'Minhad, K., & Ali, K. (2022). Advancements of wind energy conversion systems for low-wind urban environments: A review. *Energy Reports*, 8, 3406-3414. <https://doi.org/10.1016/j.egy.2022.02.153>
- Tummala, A., Velamati, R. K., Sinha, D. K., Indrāja, V., & Krishna, V. H. (2016). A review on small scale wind turbines. *Renewable Sustainable Energy Reviews*, 56, 1351-1371. <https://doi.org/10.1016/j.rser.2015.12.027>
- White, L., & Wakes, S. (2014). Permitting best use of wind resource for small wind-turbines in rural New Zealand: A micro-scale CFD examination. *Energy for Sustainable Development*, 21, 1-6. <https://doi.org/10.1016/j.esd.2014.04.003>
- Wilberforce, T., Olabi, A., Sayed, E. T., Alalmi, A. H., & Abdelkareem, M. A. (2023). Wind turbine concepts for domestic wind power generation at low wind quality sites. *Journal of Cleaner Production*, 394, 136137. <https://doi.org/10.1016/j.jclepro.2023.136137>
- Wu, Q., & Sun, Y. (2018). *Modeling and modern control of wind power*. John Wiley & Sons. ISBN: 978-1-119-23626-9; <https://www.wiley.com/en-br/Modeling+and+Modern+Control+of+Wind+Power-p-9781119236399>



© 2023. The Author(s). This article is an open access article distributed under the terms and conditions of the Creative Commons Attribution-ShareAlike 4.0 (CC BY-SA) International License (<http://creativecommons.org/licenses/by-sa/4.0/>)